

Magnetism of Cold Fermionic Atoms on p-Band of an Optical Lattice

Lei Wang¹, Xi Dai¹, Shu Chen¹, and X. C. Xie^{2,1}

¹*Beijing National Lab for Condensed Matter Physics and Institute of Physics,
Chinese Academy of Sciences, Beijing 100080, China*

²*Department of Physics, Oklahoma State University, Stillwater, Oklahoma 74078, USA*

We carry out *ab initio* study of ground state phase diagram of spin-1/2 cold fermionic atoms within two-fold degenerate p -band of an anisotropic optical lattice. Using the Gutzwiller variational approach, we show that a robust FM phase exists for a vast range of band fillings and interacting strengths. The ground state crosses over from spin density wave state to spin-1 Neel state at half filling. Additional harmonic trap will induce spatial separation of various phases. We also discuss several relevant observable consequences and detection methods. Experimental test of the results reported here may shed some light on the long-standing issue of itinerant ferromagnetism.

PACS numbers: 03.75.Ss, 03.75.Mn, 71.10.Fd, 05.30.Fk

Introduction: Recently, research of ultracold atomic gases have simulated a new wave of studying the many-body problems. One can create periodic potentials to confine the ultracold atoms by intersecting laser beams. Because of the experimental controllability of atom number, dimensionality, geometry as well as interaction strength *etc.*, the optical lattice provides an ideal playground for investigating many body problems. Specifically, the experimental realization of a Mott-insulator phase transition in the optical lattice [1][2] brings us to the forefront of the strongly correlated systems. More recently, the experimental progress makes it possible to put fermions into the optical lattices and control the interaction between them [3][4]. These advances open a new channel to investigate numerous phenomena that play important roles in the condensed matter physics, such as quantum magnetism [5][6][7], high-temperature superconductivity[8] and physics associated with band degeneracy [9][10].

Itinerant ferromagnetism in transition metals is another controversial issue in condensed matter physics. Despite long history dating back to Stoner [12], a fully understanding of its mechanism is still lacking [13]. However, a consensus is reached that the appearance of robust ferromagnetism is not a generic feature of the single band Hubbard model in a cubic lattice. *Non-bipartite* lattice structures may stabilize FM order, degenerate bands and the Hund' rule coupling may also help. Testing various scenarios using the ultra-cold fermionic atoms in optical lattice may shed light on this issue. The highly tunable and neatness of cold atom experiments also permit calculations with no adjustable parameters, the phase diagram and experimental signatures could be determined through the following first principle parameters: the depth of the optical lattice \mathbf{V} for each directions and the s -wave scattering length a_s .

In this paper, we first perform band structure calculations to identify a parameter region of \mathbf{V} and a_s where fermionic atoms on an optical lattice could be effectively described by a two-band Hubbard model. Band calcu-

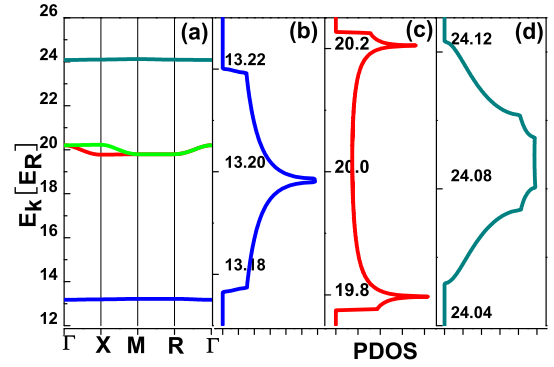


FIG. 1: (a). Band structures of four low lying bands (s , p_x , p_y and p_z) of an optical lattice with $V_x = V_y = 16E_R$, $V_z = 36E_R$. (b)-(d). Projected density of states (PDOS) for each band. The bandwidth of p_x and p_y band (c) is about 10 times wider than the s -band (b), due to the large overlap of p -band atomic wave function. The low lying s -band shows 2D characterizes, while PDOS of p_x and p_y band are degenerate and show quasi-1 dimension characterizes. A weakly breaking of the particle-hole symmetry also could be recognized from the asymmetry of the PDOS. Interestingly, the PDOS of p_z -band has 3D characterizes (d), this is due to the strength of σ -bond along z -axis is strongly suppressed by large V_z and becomes comparable to the weak π -bond along x and y directions.

lation also provides effective coupling strengths of the model. We then obtain zero temperature phase diagram as function of the coupling strength and the density of fermionic atoms by applying Gutzwiller variational approach. Finally, we consider the effect of external harmonic trap within the local spin density approximation (LSDA), which is shown to induce concentric shell structures of different phases. In particular, a robust ferromagnetic shell composed of spin polarized fermions emerges.

The model and the band structure calculations: Six counter-propagating lasers generate potential of the form $V(\mathbf{r}) = V_x \sin^2(k_L x) + V_y \sin^2(k_L y) + V_z \sin^2(k_L z)$. Atoms trapped by this potential form a simple cubic lattice with

lattice spacing $a = \frac{\pi}{k_L}$. Fig.1 shows the band structures of the optical lattices with $V_x = V_y = 16E_R, V_z = 36E_R$, where $E_R = \frac{\hbar^2 k_L^2}{2m}$ is the recoil energy. The degenerate p_x and p_y -band are well separated from the low lying s -band, p_z band are pushed up by the large V_z . Assuming the s -band is fully occupied, as long as the band gaps are much larger than the interaction scales within each band, we can focus on the degenerate p_x and p_y bands. Authors of [14] assume that atoms mainly interact in the p-wave channel thus could be effectively treat as spinless fermions and they studied effects of different lattice structures. In the present study, we focus on cubic lattice and consider the s-wave pseudo-potential $V(\mathbf{r} - \mathbf{r}') = \frac{4\pi\hbar^2 a_s}{M} \delta(\mathbf{r} - \mathbf{r}')$, which makes the problem more relevant to condensed matter system where spin 1/2 fermions plays the main role. Neglect all interaction terms except the largest on-site one, we introduce an effective two-band Hubbard model on cubic lattices:

$$\begin{aligned}
H &= H_{kin} + H_{int} \\
H_{kin} &= \sum_{\mathbf{k}, \alpha, \sigma} \varepsilon_{\mathbf{k}\alpha} \hat{c}_{\mathbf{k}\alpha\sigma}^\dagger \hat{c}_{\mathbf{k}\alpha\sigma} + h.c. \\
H_{int} &= U \sum_{i\alpha} \hat{n}_{i\alpha\uparrow} \hat{n}_{i\alpha\downarrow} + U' \sum_{i\sigma} \hat{n}_{i\alpha\sigma} \hat{n}_{iy\sigma} \\
&+ J \sum_{i\alpha} (\hat{c}_{i\alpha\uparrow}^\dagger \hat{c}_{i\bar{\alpha}\downarrow}^\dagger \hat{c}_{i\alpha\downarrow} \hat{c}_{i\bar{\alpha}\uparrow} + \hat{c}_{i\alpha\uparrow}^\dagger \hat{c}_{i\alpha\downarrow}^\dagger \hat{c}_{i\bar{\alpha}\downarrow} \hat{c}_{i\bar{\alpha}\uparrow}) \quad (1)
\end{aligned}$$

With

$$\begin{aligned}
U &= \frac{4\pi\hbar^2 a_s}{M} \int d\mathbf{r} w_x(\mathbf{r})^4 \\
U' &= J = \frac{4\pi\hbar^2 a_s}{M} \int d\mathbf{r} w_x(\mathbf{r})^2 w_y(\mathbf{r})^2 \quad (2)
\end{aligned}$$

where $\alpha = x, y$ is the band index, $\sigma = \uparrow, \downarrow$ denote spins, $\varepsilon_{\mathbf{k}\alpha}$ is energy dispersion for each band. a_s is the s-wave scattering length which could be tuned by Feshbach resonance technique over a large scope of magnitude. We only consider repulsive interaction ($a_s > 0$) in this study. Parameter U describes the on-site Coulomb repulsive interaction between atoms reside in the same orbital, while U' describes the repulsive interaction for two atoms in different orbitals. J controls the strength of Hund's rule coupling between different orbitals. In the present system only transverse part of the Hund's rule coupling survives, *i.e.* the spin flip and pair hopping processes. The absence of the density-density interaction for atoms with the same spins is due to the short range δ type pseudo-potential. This fact can also be understood as a fully canceling between the longitudinal part of the Hund's rule coupling and corresponding terms in the inter-orbital density-density interactions. All of the interaction parameters are expressed as overlaps of maximally localized Wannier functions[15].

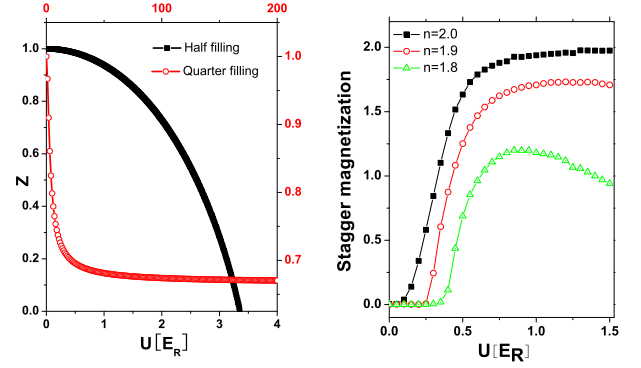


FIG. 2: (a). Quasi-particle weight v.s. interaction strength U . U' and J are varied with U by keeping $U' = J = 0.299U$. At quarter filling (Red hollow dot) the quasi-particle weight saturate to nonzero value, indicating an absence of the Brinkman-Rice transition. (b). Stagger magnetization v.s. interaction strength for several different fillings. At half filling ($n = 2$) the system crossover from weak coupling SDW behavior to strong coupling spin-1 Neel state. Away from half filling, it's needed a finite interaction strength to induce stagger magnetization.

Both the band dispersions $\varepsilon_{\mathbf{k}\alpha}$ and the coupling constants in Eq. 2 are determined by experimentally controllable parameters \mathbf{V} and a_s . Due to the anisotropic nature of the p-orbitals, the system shows dimension reduction behavior: the PDOS has Van Hove singularity near the band edge resembling of 1D character. This feature is also included by the tight binding model with an anisotropic hopping amplitude along different directions[16]. At half filling, the Fermi surface has nesting property with the nesting vector (π, π, π) [17]. In contrast to the isotropic case (s-band), here the singularity in PDOS and Fermi surface nesting occur at separable energy scales and lead to remarkable consequence: instability towards to different magnetic orders dominates at different fillings. For the given lattice depth $V_x = V_y = 16E_R, V_z = 36E_R$, our calculation shows the bandwidth W of the two-fold degenerate p -band is $0.45E_R$, while band gaps separated p_x, p_y -bands with s and p_z -bands are $6.79E_R$ and $4.10E_R$ (Fig.1(b)). Overlap of Wannier functions gives $U/E_R = 8.63k_L a_s$ and $U' = J = 0.299U$, while the interaction scale within s-band is $13.1(k_L a_s)E_R$. Not exceeding the band gaps pose 0.0755λ as the upper limit for a_s . Within this restriction, one could still tune the system from weak to strong coupling ($U \sim 9W$) region by Feshbach resonance technique.

Gutzwiller variation results: For this complex two-band Hubbard model we adopt a generalized version of the Gutzwiller variational approach [18][19][20][21][22]. Historically, the variational approach has been successfully used to treat strong correlated systems such as normal ^3He [23] and Mott transition [24]. Generalization of it is used to investigate physics associate with band degeneracy, such as orbital selective Mott transi-

tion [20][25] and transition metal ferromagnetism [21]. The variational wave function is $|\Phi_G\rangle = P_G|0\rangle$, where $|0\rangle$ is uncorrelated state which could be fermi liquid, spin density wave or superconductivity ground state. And $P_G = \prod_i \sum_{\Gamma} \lambda_{i,\Gamma} m_{i,\Gamma}$, $m_{i,\Gamma}$ are projection operator onto atomic configurations, $\lambda_{i,\Gamma}$ are corresponding variational parameters. Under Gutzwiller approximation (GA) [18][23] one can evaluate expected values of operators over the projected wave function. By minimizing the total energy one gets the ground state configurations, from which one can identify various orders *e.g.*, charge density wave order, orbital order, FM and AF order *etc.* GA neglects spatial correlations and is only exact in infinite dimension, this approximation has also been proven to be equivalent to the saddle point of Kotliar-Ruckenstein slave boson functional treatment[26]. Since it is non-perturbative in nature, the variational approach treats the Fermi liquid as well as Mott localized state on equal footing and hence gives a coherent description of the intermediate coupling strength, connecting the weak coupling mean field to the strong coupling perturbation results[17]. And the result of the present method is superior to Hartree-Fock mean field that often overestimates the tendency towards the ordered phases.

Disregard any long range order, at commensurate filling a reasonable large on-site repulsive interaction would localize fermions and drive the system into the paramagnetic Mott insulator phase. The transition (Brinkman-Rice transition) could be described naturally within Gutzwiller variational approach [24] via quasi-particle weight Z , which contributes to the coherent peak in the spectral function. It could also be interpreted as the renormalization factor of kinetic energy, the height of Fermi step or inverse of mass enhancement factor. As Z approaches to zero, fermions becomes more and more localized and finally transforms into the Mott insulator phase. However in the present case the large Hund's rule coupling $J = U'$ has dramatic effect on the paramagnetic Mott transition: there is no Brinkman-Rice transition at quarter filling, see Fig.2(a). The on-site interaction Hamiltonian Eq.1 has doubly occupied spin-triplet as its lowest energy states, which are degenerate with the empty and singly occupied states. Charge fluctuation through this channel is allowed at quarter filling thus the system does not become localized when U increases. At half filling this kind of fluctuation is blocked by the large on-site intra-orbital repulsive interaction U and the Brinkman-Rice transition manifests itself as shown in Fig.2(a). However because of the huge spin entropy of the paramagnetic Mott state, it would not act as the ground state at zero temperature. When the system cools down the degeneracy will be lifted and various magnetic/orbital orders develop depending on the residual interactions between the spin/orbital degrees of freedom.

Next we discuss the magnetic order of the p-band

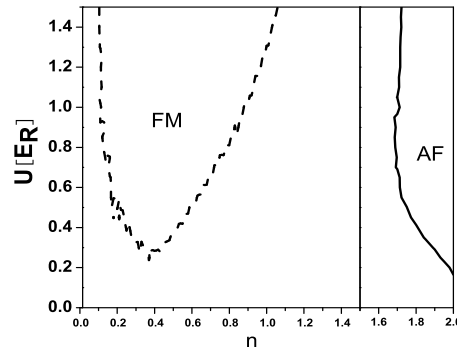


FIG. 3: Ground state phase diagram. Region enclosed by full and dashed line is antiferromagnetic and ferromagnetic phases respectively, the remainder part is in paramagnetism phase. Contrary to the single band case, there is robust ferromagnetic phase for vast range of filling and coupling strength.

fermions. As the previous section indicated, the band structure (Fermi surface nesting and the Van Hove singularity) favors AF and FM order at different energy scales, and the on-site Hund's rule coupling may help stabilizing them. Thus, it is possible that these two phases may exist even for weak or intermediately coupling strength. And it is interesting to observe the coexistence of them in the optical lattices with an external harmonic trap.

Fig. 2(b) shows the development of the stagger magnetization with increase of U near half filling ($n = 2$). Due to the Fermi surface nesting, an arbitrary small U drives the instability of the two-sublattice antiferromagnetism at exact half filling. At weak coupling it follows the spin density wave mean field prediction, the stagger magnetization increases as $te^{-t/U}$. Approaching the strong coupling limit the stagger magnetization comes to its saturation value 2. In this limit, the large repulsive interaction quenches the charge degree of freedom while the on-site Hund's rule coupling locks the local spins to form spin-1 moments. Virtual hopping process leads to the antiferromagnetic coupling of these local moments and the original fermions model reduces to a spin-1 antiferromagnetic Heisenberg model. This high spin AF order is more stable against the quantum fluctuations. The present method also gives a coherent description of the weak to strong crossover region, where the stagger magnetization shows non-monotonic behavior for $n = 1.8$ as shown in Fig.2(b). The condensation energy of AF order is roughly W^2/U , which is 10 times larger than the s -band, see Fig.1(b)(c). Due to the large energy gain of the antiferromagnetic order, we anticipate the transition temperature to be two orders higher than that of the s -band case at the strong coupling limit. At intermediate coupling strength the transition temperature may attain its maximum value, which is accessible in current cold atomic experiments.

Upon doping, the AF order is destroyed by movement

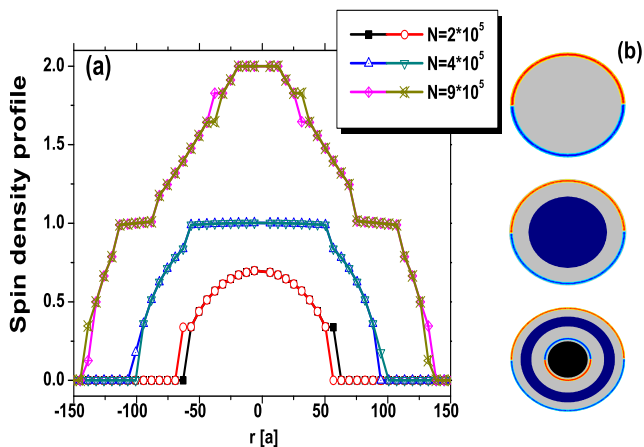


FIG. 4: (a). Side view of spin density profile in a harmonic trap with different total number of atoms, two spin state are 50 : 50 mixture. The frequency of the external trap is $\Omega = 0.005 E_R$. (b). Top view of various phases. Dark Blue region denotes antiferromagnetic phases, Black region denotes band insulator and shallow blue/red for two kinds of polarized fermions(ferromagnetic phase). Only density of atoms on the p-band are shown in the figure, s-band spin densities provides a homogeneous background near the center of the trap.

of holes and the system has featureless PM ground state. But at even lower fillings where the Van Hove singularity plays a role the system has FM ground state. Actually for the present depth of optical lattice, the singularity in DOS plays the main role and the Hund's rule coupling further stabilizes the tendency and enlarges the region of FM order in the phase diagram. It is possible to tune the optical lattice to change the relative weight of contribution of singularity in DOS and the Hund's rule coupling, and this will shed light on the long controversial issue of the mechanics of ferromagnetism in the transition metal oxides. Due to the approximately particle-hole symmetry of the DOS, the phase diagram shows a mirror symmetry with the $n = 2$ axis, *i.e.*, there is a FM region of similar shape at higher fillings.

We now come to the effect of the external confinement. It is provided by a combination of the magnetic trap and the Gaussian profile of the laser beams. Combing with the local spin density approximation(LSDA), our Gutzwiller variational approach provides a natural way of incorporating spatial inhomogeneities into the treatment of strong correlations. According to the celebrated Hohenberg-Kohn theorem [27], the ground state energy of an inhomogeneous system is solely determined by its ground state spin density distribution.

$$E^{tot} = \int d\mathbf{r} \{ E^{kin+int}[n_{\uparrow}(\mathbf{r}), n_{\downarrow}(\mathbf{r})] + V^{ext}(n_{\uparrow}(\mathbf{r}), n_{\downarrow}(\mathbf{r})) \} \quad (3)$$

where $E^{kin+int}[n_{\uparrow}(\mathbf{r}), n_{\downarrow}(\mathbf{r})]$ includes the kinetic energy, the lattice potential and the interaction energy of fermions on an optical lattice, which depends on the spin density distribution non-locally in general.

$V^{ext}(n_{\uparrow}(\mathbf{r}), n_{\downarrow}(\mathbf{r})) = \frac{1}{2} \Omega^2 r^2 (n_{\uparrow}(\mathbf{r}) + n_{\downarrow}(\mathbf{r}))$ is the trap energy. Usually Ω is much smaller compare to the characteristic frequency of the optical lattice, thus the trap provides a spatially slowly varying chemical potential. We could expand the functional to the lowest order: $E^{kin+int}[n_{\uparrow}(\mathbf{r}), n_{\downarrow}(\mathbf{r})] \approx E^{kin+int}(n_{\uparrow}(\mathbf{r}), n_{\downarrow}(\mathbf{r}))$, where the functional dependence on local spin densities could be obtained by previously Gutzwiller variational calculation. Physical picture of this strategy (LSDA) is to divide the whole system into mesoscopic clusters of size $l_{\Omega} = \sqrt{\frac{\hbar}{M\Omega}}$. Each of them feels homogeneous external potential and at the same time could be treated as in the thermodynamic limit, and Gutzwiller variational study gives the dependence of energy and local spin densities within each cluster.

We perform optimization of E^{tot} by varying over spin density distributions for $U = 0.6 E_R$ (U' and J are determined correspondingly) and several total number of atoms, the results are shown in Fig. 4. Densities of both spins decrease from the trap center continuously to zero at the trap edge because of the external potential. Due to the orbital degeneracy, maximum filling at the trap center is 2 for each spin, forming band insulator phases. Competition of the external potential and cohesive energy of the ordered phase gives fine structures of spin density profiles. Regions where spin density around 1 are more likely to enter into AF phase, as long as the energy gain from AF phase exceeds correspondingly energy loss from density redistribution. Plateaus formed by AF (or PM Mott Insulator) phase was also reported in previous Quantum Monte Carlo [28] and Dynamical Mean Field theory [29] study on single band inhomogeneous cold fermionic atom systems. For regions with average filling less than 0.5 or larger than 1.5 there are tendency towards ferromagnetic order. But due to the conservation of total spins, FM region will consist of two domains of half-shell shape with opposite spin polarization, see Fig.4(a), similar structure is anticipated in [30] concerns Nagaoka ferromagnetism. To sum up, p-band cold fermionic atoms will form shell structures with an external trap potential, for different radii the system crosses the $U - n$ phase diagram and shows an band insulator, PM, FM and AF phases Fig. 4(b).

Experimental signatures: Population of higher bands have been detected by time of flight (TOF) images [3][31]. Noise correlation [32][33] from TOF images may also detect spin order through spin-spin correlation functions. Specifically, AF phase opens a charge transfer gap which could be detected by Raman spectroscopy [34], while the doubling of unit cell might be detected by spin selective Bragg spectroscopy [35]. Spatial distribution of spin densities in harmonic trap reported in this paper could be detected by spatially microwave transition and spin-changing collisions techniques, which measure the integrated density profiles along chosen directions [36].

Summary: Combining the band structure calculations and the Gutzwiller variational approach, we perform a first principle calculation of the zero temperature phase diagram of spin-1/2 cold fermionic atoms on the two-fold degenerate p-band in an optical lattice. We show that the system has robust ferromagnetic and antiferromagnetic ground state at different fillings. We have traced back the physical picture to the single particle feature included anisotropy of orbital orientations and Fermi surface nesting as well as correlated effects such as Hund' rule coupling. We also discuss the inhomogeneous spatial distribution induced by an external harmonic potential.

Acknowledgement: The work is supported by NSFC. Xie is supported by US-DOE and NSF.

-
- [1] D. Jaksch, C. Bruder, J. I. Cirac, C. W. Gardiner and P. Zoller. Phys. Rev. Lett. **81**, 3108 (1998).
- [2] M. Greiner, O. Mandel, T. Esslinger, T. W. Hansch and I. Bloch. Nature. **415**, 39 (2002).
- [3] M. Köhl, H. Moritz, T. Stoferle, K. Gunter and T. Esslinger. Phys. Rev. Lett. **94**, 080403 (2005).
- [4] R. Jördens, N. Strohmaier, K. Günter, H. Moritz and T. Esslinger, arXiv:0804.4009
- [5] F. Werner, O. Parcollet, A. Georges and S. R. Hassan, Phys. Rev. Lett. **95**, 056401 (2005).
- [6] L. M. Duan, E. Demler, and M. D. Lukin, Phys. Rev. Lett. **91**, 090402 (2003).
- [7] S. Trebst, U. Schollwöck, M. Troyer and P. Zoller, Phys. Rev. Lett. **96**, 250402 (2006).
- [8] W. Hofstetter, J. I. Cirac, P. Zoller, E. Demler and M. D. Lukin, Phys. Rev. Lett. **89**, 220407 (2002).
- [9] R. B. Diener and T. L. Ho, Phys. Rev. Lett, **96**, 010402 (2006).
- [10] A. F. Ho, Phys. Rev. A, **73**, 061601(R) (2006).
- [11] T. Müller, S. Fölling, A. Widera and I. Bloch, Phys. Rev. Lett. **99**, 200405 (2007)
- [12] E. C. Stoner, Rep. Prog. Phys. **11**, 43 (1946).
- [13] S. Sakai, R. Arita, and H. Aoki, Phys. Rev. Lett **99**, 216402 (2007).
- [14] Congjun Wu, D. Bergman, L. Balents, and S. Das Sarma, Phys. Rev. Lett. **99**, 070401 (2007); C. J. Wu, arXiv:0801.0888; E. Zhao and W. V. Liu, Phys. Rev. Lett. **100**, 160403 (2008); Congjun Wu and S. Das Sarma, arXiv:0712.4284
- [15] N. Marzari and D. Vanderbilt, Phys. Rev. B. **56**, 12847 (1997).
- [16] W. V. Liu and C. J. Wu, Phys. Rev. A. **74**, 013607 (2006).
- [17] K. Wu and H. Zhai, arXiv:0710.3852.
- [18] M. Gutzwiller, Phys. Rev. Lett. **10**, 159 (1963), and Phys. Rev. **137**, A1726 (1965).
- [19] J. Bünemann, W. Weber and F. Gebhard, Phys. Rev. B. **57**, 6896 (1998).
- [20] X. Dai, G. Kotliar and Z. Fang, cond-mat/0611075.
- [21] R. Frésard and G. Kotliar Phys. Rev. B. **56**, 12909 (1997).
- [22] X. Y. Deng, X. Dai and Z. Fang, arXiv:0707.4606.
- [23] D. Vollhardt, Rev. Mod. Phys. **56**, 99 (1984).
- [24] W. F. Brinkman and T. M. Rice, Phys. Rev. B **2**, 4302 (1970).
- [25] A. Koga, N. Kawakami, T. M. Rice and M. Sgrist, Phys. Rev. Lett. **92**, 216402 (2004).
- [26] G. Kotliar and A. E. Ruckenstein, Phys. Rev. Lett. **57**, 1362 (1986).
- [27] H. Hohenberg and W. Kohn, Phys. Rev. **136**, B864 (1964).
- [28] M. Rigol, A. Muramatsu, G. G. Batrouni and R. T. Scalettar, Phys. Rev. Lett. **91**, 130403 (2003); M. Rigol and A. Muramatsu, Phys. Rev. A. **69**, 053612 (2004).
- [29] M. Snoek, I. Titvinidze, C. Toke, K. Byczuk and W. Hofstetter, arXiv:0802.3211; R. W. Helmes, T. A. Costi and A. Rosch, Phys. Rev. Lett. **100**, 056403 (2008).
- [30] H. Park, K. Haule, C. A. Marianetti, and G. Kotliar, Phys. Rev. B **77**, 035107 (2008)
- [31] T. Müller, S. Fölling, A. Widera and I. Bloch, Phys. Rev. Lett. **99**, 200405 (2007).
- [32] E. Altman, E. Demler, and M. D. Lukin, Phys. Rev. A. **70**, 013603 (2004).
- [33] S. Fölling, F. Gerbier, A. Widera, O. Mandel, T. Gerlcke, and I. Bloch, Nature. **434**, 481 (2005).
- [34] T. L. Dao, A. Georges, J. Dalibard, C. Salomon, and I. Carusotto, Phys. Rev. Lett. **98**, 240402 (2007).
- [35] I. Barusotto, J. Phy. B: At. Mol. Opt. Phys, **39**, S211 (2006).
- [36] S. Fölling, A. Widera, T. Müller, F. Gerbier, and I. Bloch, Phys. Rev. Lett. **97**, 060403 (2006).